Pediatr Surg Int (2005) 21: 615–620
DOI 10.1007/s00383-005-1483-9

ORIGINAL ARTICLE

Regina Y. Y. Chan · Carolyn E. L. Tan
Gerard Czech-Schmidt · Claus Petersen

Computerized three-dimensional study of a rotavirus model of biliary atresia: comparison with human biliary atresia

Accepted: 8 June 2005 / Published online: 2 August 2005

Abstract Biliary atresia is a panbiliary disease causing obstructive jaundice in neonates and infants. The clinical spectrum can be broadly categorized into the fetal and perinatal types. A consistent animal model that accurately mimics the whole clinical spectrum of biliary atresia is not yet available. However, rotavirus infection of neonatal mice has been shown to produce atresia in the biliary system. This study investigates the three-dimensional computerized morphology of the murine neonatal model comparing with age-matched control mice. Newborn Balb/c mice were injected intraperitoneally with rhesus rotavirus within 24–48 h after birth. Control mice received 0.9% NaCl. Pups with symptoms of cholestasis were sacrificed from the 5th to the 15th postinjection day, as were age-matched controls. Their hepatobiliary tissues were prepared for three-dimensional computerized image reconstruction. Rotavirus infection caused obliteration of the intrahepatic bile ducts and single to multiple atresias in the extrahepatic bile duct. At 15 days postinjection, intrahepatic ductal proliferation appeared, and the three-dimensional appearances of the intrahepatic biliary structures were similar to the human disease. Cystic duct and gallbladder dilatation was frequently seen in this model, and this feature distinguishes it from the human disease in which the gallbladder is almost always atretic. This rotavirus murine model demonstrates many of the features of human perinatal biliary atresia, and can be used as an investigative tool to further study the pathogenesis of biliary atresia.

Keywords Biliary atresia · Animal model · Rotavirus

R. Y. Y. Chan · C. E. L. Tan
Department of Pediatric Surgery, KK Women's and Children's Hospital, 100 Bukit Timah Road, Singapore 229899

G. Czech-Schmidt · C. Petersen
Department of Pediatric Surgery, Hannover Medical School, Carl-Neuberg-Strasse 1, 30625 Hannover, Germany

R. Y. Y. Chan (✉)
Department of Medicine, National University of Singapore, NUH Main Building # 03-31, 5 Lower Kent Ridge Road, Singapore 119074
E-mail: ryychan@singnet.com.sg
Fax: +65-6779-4112

Introduction

Biliary atresia (BA) is an obliterative disorder of the extrahepatic and intrahepatic bile ducts (IHBD) that affects 1 in 8,000 to 1 in 15,000 live births, and is the most frequent indication for liver transplantation in children [1]. The precise etiology of BA is still uncertain, although viral infection, toxic insults, immunologic mechanisms, and failure of ductal plate remodeling have been postulated [2].

The role of several hepatotrophic viruses in the etiology of BA has been examined, but no single causative agent has been identified so far. However, intraperitoneal injection of group A rotavirus into newborn Balb/c mice produced irreversible extrahepatic biliary obstruction after 2 weeks, with histological findings similar to that found in children with BA by the third to fourth week of life [3, 4]. With the use of scanning electron microscopy, a wide range of morphological findings could be demonstrated in the extrahepatic bile ducts [5], but information on the intrahepatic ducts was limited to just histological assessment of serial sections.

In the present study, we have applied the technique of computerized three-dimensional (3D) reconstruction to systematically investigate the morphology of the intrahepatic and extrahepatic bile ducts in the group A rotavirus-infected newborn Balb/c mouse model, and compared the features with the human disease [6]. In this study we focused on the early phase of the model, in order to study the sequence of events leading to subsequent development of bile duct atresia in rotavirus-infected mice and to improve our understanding of its pathogenesis.

Materials and methods

Animals

Newborn Balb/c mice were infected within 24–48 h of birth, as described in a previous study [5]. Briefly, 10 µl of 30% glucose solution—containing $\sim 10^4$ pfu/ml of rhesus rotavirus (strain MMU 18006)—was diluted in 20 µl 0.9% NaCl and injected intraperitoneally. Control mice received 30 µl 0.9% NaCl. From the 5th to the 15th day postinfection (p.i.), pups with symptoms of cholestasis and the corresponding control mice were sacrificed. The specimens, containing the porta hepatis, hepatoduodenal ligament, gallbladder, and a part of the duodenum, were fixed in formalin and embedded in paraffin. This animal study complied with the national regulations for protection of animals and was under the supervision of the veterinarian of the responsible institute (Permit no. 98/72, Bezirksregierung, Hannover, Germany).

Histochemistry

Five micrometer (µm) serial sections were cut from each paraffin block, and every third section was stained with routine Hematoxylin and Eosin. To aid identification of the biliary structures, immunohistochemistry was carried out on separate sections with a cytokeratin antibody, clone AE1/AE3, and detected using an Animal Research Kit (both from Dako, USA). Tissue sections were cleared in xylene and rehydrated through graded dilutions of alcohol. Epitope retrieval consisted of a 30-min incubation with ready-to-use proteinase K (Dako, USA) at room temperature. Prior to each step in the procedure, the slides were rinsed in phosphate-buffered saline. To block endogenous peroxidase activity, sections were incubated with 0.03% hydrogen peroxide for 5 min, while endogenous avidin-binding activity was suppressed by sequential 10-min incubations with avidin and biotin (Avidin/Biotin Blocking Kit, Vector Laboratories, USA). The primary antibody (1:50 dilution) was labeled with a biotinylated Fab secondary antibody as per manufacturer's instructions and incubated with the tissue sections for 15 min at room temperature. The slides were next incubated with streptavidin-peroxidase for 15 min and visualized by the addition of 3′3-diaminobenzidine (DAB) chromogen-substrate. Finally, the sections were counterstained in hematoxylin, dehydrated and mounted using DePeX (BDH, England). Negative controls were run in parallel omitting the primary antibody.

Image analysis

The stained sections were digitized for 3D reconstruction through a CCD camera (ProgRes 3012, Kontron Elektronik, Germany) that was attached to a microscope (Axiophot, Carl Zeiss, Germany). Using the KS300 3.0 Imaging System software (Carl Zeiss, Germany), the sections were aligned by converting the preceding image to an overlay, and aligning the current slide using the rotation stage of the microscope according to the overlay. All images were acquired using a 2.5× NA 0.075 objective lens, at a resolution of 1024×774 pixels (5 µm/pixel). Lumens of the biliary structures in each image were then manually traced and saved as binary images. Since every third section of each specimen was used for the 3D reconstruction, the images had to be replicated three times to ensure volumetric accuracy. Images were stored as TIFF files prior to 3D reconstruction.

3D reconstruction

The images collected for each specimen were rendered as individual datasets in VoxBlast 3.1 (VayTek, USA), a 3D visualization and measurement software. The rendered 3D image could be rotated in any direction and the post-rendering lighting model was used to apply shadowing effects to the image. Specimens from nine rotavirus-infected and six control mice were reconstructed.

Results

In this study, we have systematically investigated the biliary system of control and rhesus rotavirus (strain MMU 18006)-infected Balb/c mice using computerized 3D reconstruction of serial 5 µm histological sections of the livers.

In control mice that were not infected with rotavirus, the biliary system was well-formed from as early as 5 days p.i. (i.e., 6 days after birth) (Fig. 1). The extrahepatic bile ducts were tubular and patent. The IHBD showed the typical branching morphology of an adult mouse, and this was consistent throughout the neonatal period until day 15 p.i.

On the other hand, in all nine liver samples from rotavirus-infected mice, atresia was observed at the distal end of the common bile duct (CBD) of which five showed segmental atresia of the proximal CBD (Figs. 1, 2, 3, 4). Prestenotic dilatation of varying sizes was seen in the CBD, cystic duct and gallbladder. Gross cystic dilatation was seen particularly at days 14 and 15 p.i., where there was complete obliteration or long segment atresia of the CBD (Figs. 5, 6). Significantly, the common hepatic duct was absent in all rotavirus-infected livers. The types of BA described generally mimicked Kasai type III [7], with the presence of cystic dilatation in some of the CBD remnants.

However in the livers of mice that were infected with rotavirus, the IHBD were few or absent until day 14 p.i. The normal branching biliary tree, as seen in the control mice, was completely lost in infected mice. At day 15 p.i.

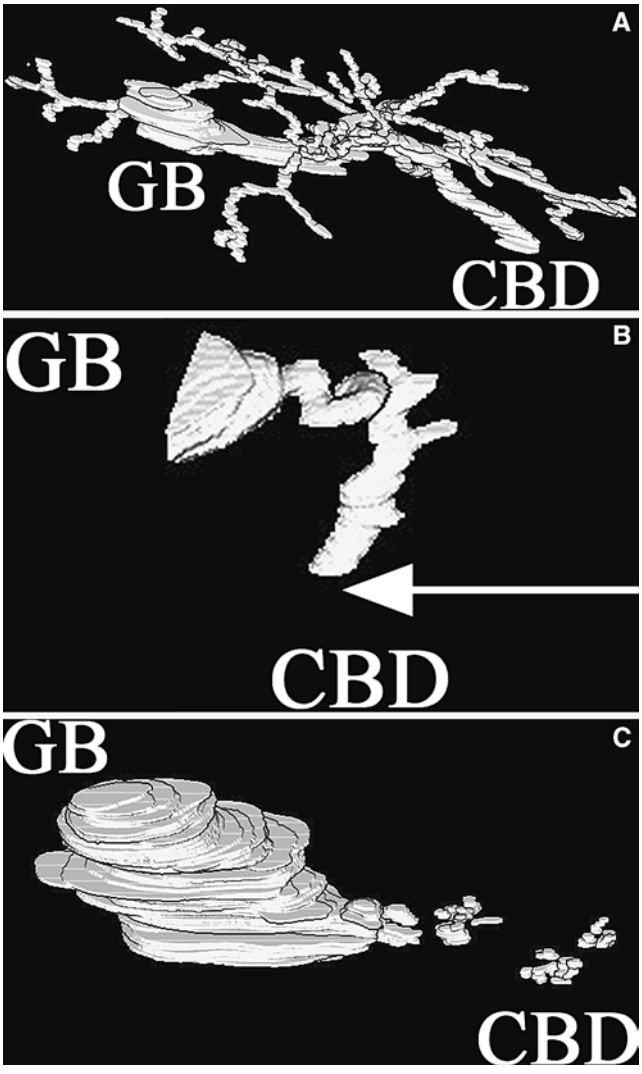

Fig. 1 3D images of biliary structures in **a** control and **b**, **c** two RRV-infected mice at 5 days postinfection (*p.i.*). In one sample (**b**), the distal part of the common bile duct (*CBD*) was destroyed (*arrow*), and slight dilatation of the gallbladder (*GB*) was observed. In another sample (**c**), multiple CBD remnants were seen and the GB was markedly dilated. Original magnification 25 times

ductal proliferation was seen, resembling the intrahepatic bile structures of human BA patients. Immunohistochemical identification of the proliferated bile ducts showed little staining as they were mostly denuded of epithelia (Fig. 7).

Discussion

Although the etiology of BA remains unknown, two forms are recognized, the *fetal* form and the more common *perinatal* form [1]. Antenatal cases, diagnosed by the presence of cystic dilatation of part of the biliary tree, have been reported [8, 9]. One postulate is that the fetal form of BA may be due to ductal plate malformation (DPM), where there is maldevelopment of the

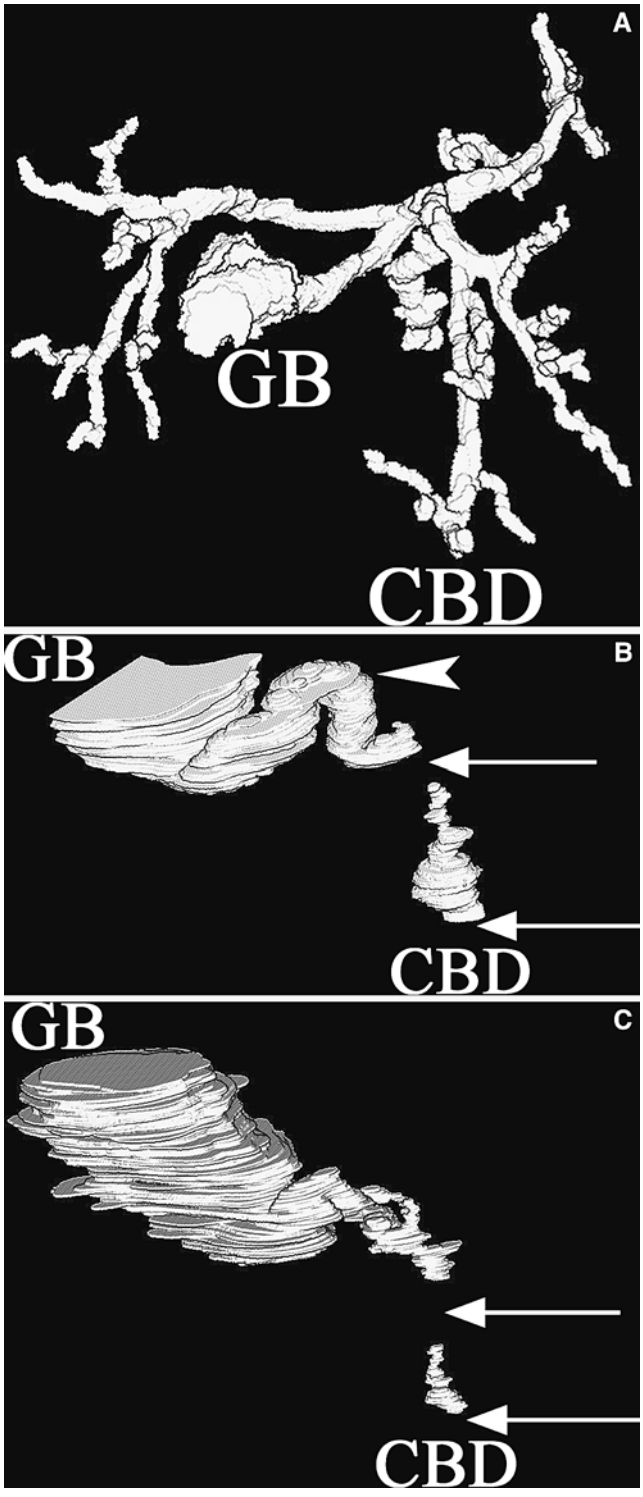

Fig. 2 3D images of biliary structures in **a** control and **b**, **c** two RRV-infected mice at 7 days p.i. In both infected mice the gallbladders (*GB*) were large, and there was segmental atresia (*long arrows*) of the CBD. Prestenotic dilatation of the CBD and cystic duct (*arrowhead*) was seen in one sample (**b**). Original magnification 25 times

fetal ductal plate into the adult-type branching biliary tree [10, 11]. Histologically, DPM is defined as the arrangement of biliary structures in an unusual

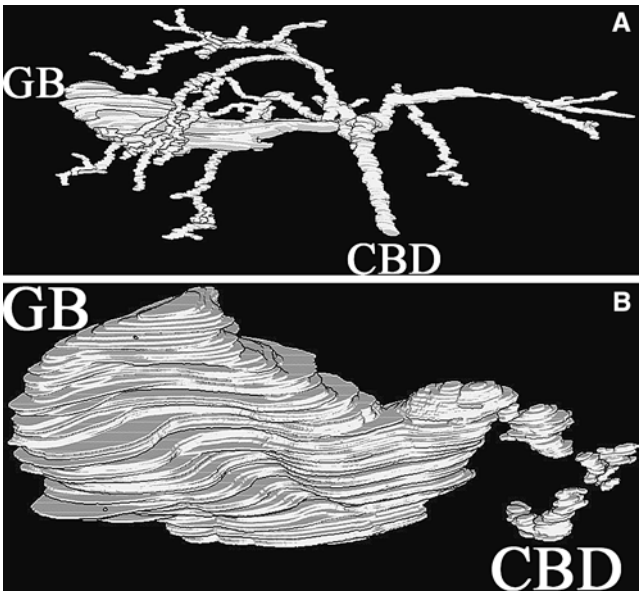

Fig. 3 3D images images of biliary structures in **a** control and **b** RRV-infected mice at 10 days p.i. Multiple areas of atresia were seen in the CBD of the infected liver. The GB was grossly dilated. Original magnification 25 times

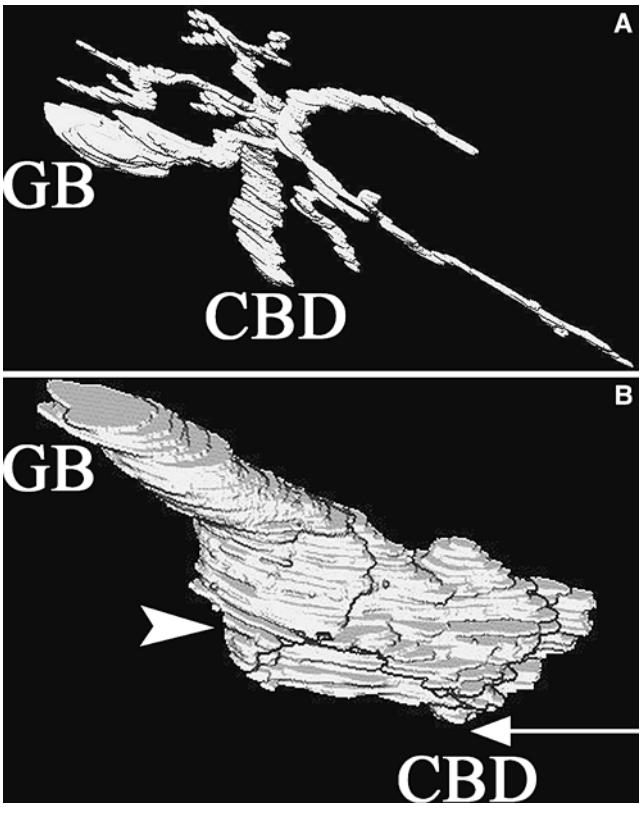

Fig. 5 3D images of biliary structures in **a** control and **b** RRV-infected mice at 14 days p.i. The entire CBD was obliterated (*long arrow*) in the infected mouse. The cystic duct (*arrowhead*) was grossly dilated and tortuous. Original magnification 25 times

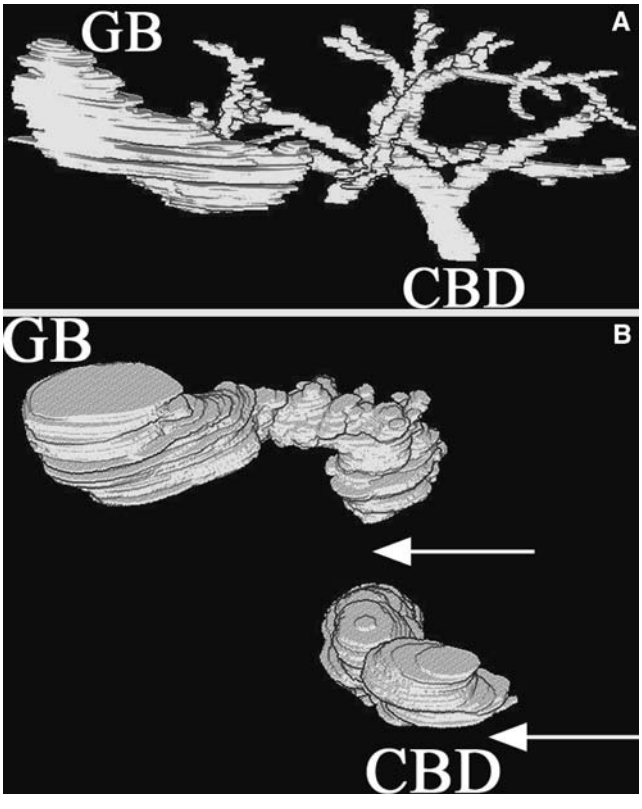

Fig. 4 3D images of biliary structures in **a** control and **b** RRV-infected mice at 12 days p.i. Atresia at the distal end of the CBD and segmental atresia at the proximal CBD were seen (*arrows*). There was dilatation of the entire biliary system. Original magnification 25 times

concentric pattern, resembling the fetal ductal plate. Its incidence varies from 21 to 38% of BA cases [12, 13], and it is believed that the disease process began in early fetal life in these patients. However, attempts at producing animal models for the antenatal form of BA have so far been unsuccessful [14, 15]. Czech-Schmidt et al. [16] reported an immunological gap of greatest vulnerability to intraperitoneal infection of newborn Balb/c mice at 12 h after birth. Antenatal infection of pregnant mice did not result in BA in the offspring, and newborn mice infected after 12 h postpartum were less affected, the older they were.

Other investigators have proposed that BA is a result of postnatal destruction of the biliary system, as indicated by the presence of bile excretion at birth. In contrast, patients with an antenatal onset of the disease have acholic stools from the first day of life. The rotavirus murine model is essentially a model of postnatally induced BA. Computerized 3D reconstruction techniques in this study showed that in control mice, the adult branching pattern of bile ducts was present in all specimens from 5 to 15 days p.i. In the rotavirus-infected mice, the IHBD were almost completely destroyed as early as 5 days p.i., with the formation of atretic segments in the extrahepatic bile ducts similar to human BA. No evidence of DPM was seen, as was

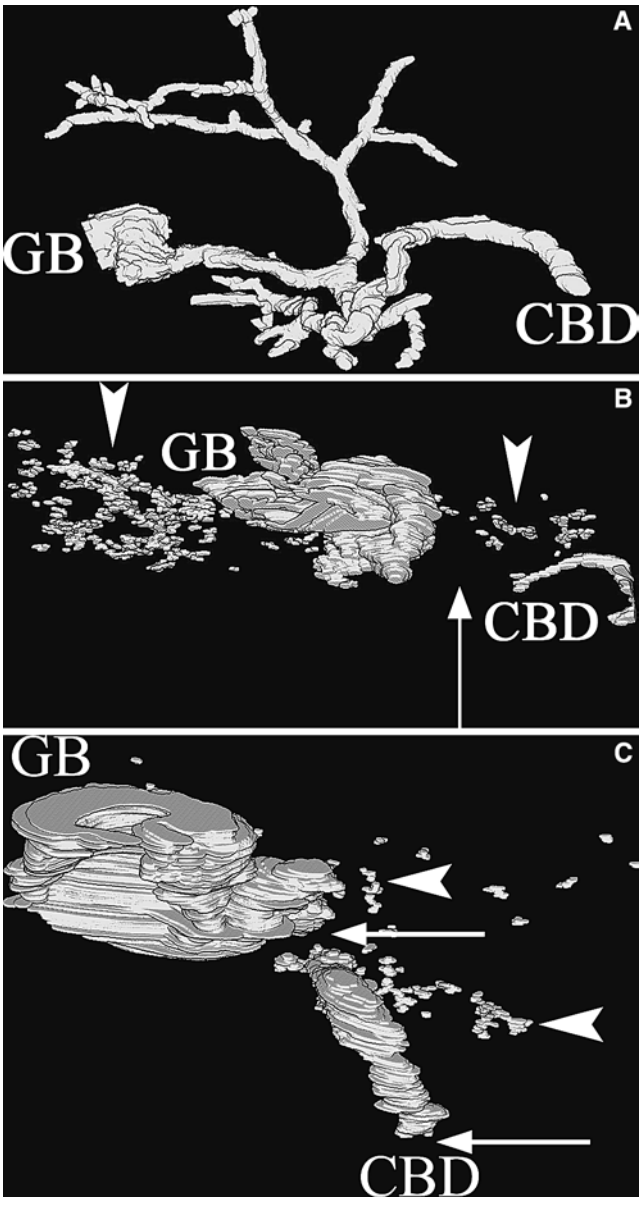

Fig. 6 3D images of biliary structures in **a** control and **b**, **c** two RRV-infected mice at 15 days p.i. Proliferation of the intrahepatic bile ducts was observed in the infected mice (*arrowheads*), more marked in one sample than the other. There was segmental atresia (*long arrows*) of the CBD, with prestenotic dilatation of the cystic duct in both infected livers. The gallbladders were collapsed. Original magnification **a**, **b** 18.75 times; **c** 25 times

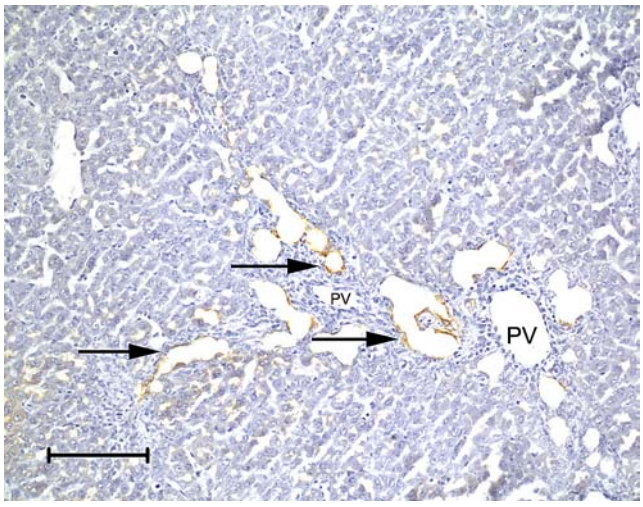

Fig. 7 Photomicrograph of a liver section from RRV-infected mouse at 15 days p.i. that has been stained with anti-cytokeratin AE1/AE3 antibody (*brown*). The bile ducts were denuded of epithelia, and ductular proliferation (*arrows*) was observed around the portal veins (*PV*). *Bar* 100 μm

expected in a postnatal model of BA. Ductular proliferation, a feature of human BA liver biopsies, was seen on 15 days p.i. in this series, though it has previously been reported to be seen after 3 weeks [3, 4]. The proliferation, as shown in Fig. 6b, bore a strong resemblance to the hepatic hilar bile ducts of human BA patients from a previous 3D study [6]. In this case, the proliferative response was probably due to bile duct regeneration from injury rather than the persistence of fetal bile ducts.

While the intrahepatic ductopenia that was seen in this model is not a common characteristic of human BA livers, Raweily et al. [12] have reported paucity of the IHBD in 6 of 37 BA patients. More recently, Azar et al. [17] described four patients with conjugated hyperbilirubinemia whose liver biopsies showed a lack of ductular proliferation, despite subsequent development of BA. Bile duct paucity is defined as a bile duct-to-portal tract ratio of less than 0.9, and can be classified into the syndromic (Alagille's syndrome) and non-syndromic forms. The above data, together with our findings from the animal model, suggest that non-syndromic bile duct paucity and BA may share a common pathogenesis but display different phenotypes. Conversely, the lack of IHBD in the animal model may represent an early manifestation of BA that is usually not seen in humans because the diagnosis is made later. Following the mouse model beyond 15 days p.i. is likely to show more prominent intrahepatic ductular proliferation. Differences in the course of the disease in humans and mice may also be due to their different immunological responses to viral infections of the hepatobiliary system.

Another striking difference from human BA was the presence of a large, distended gallbladder in the affected mice, rather than the atretic gallbladder that is often associated with BA infants [18–20]. In addition, dilatation of bile duct remnants was a prominent feature in the animal model, while this is only seen in a small portion of infants with BA. Interestingly, the degree of dilatation of the gallbladder and cystic duct appears to be related to the degree of obliteration of the CBD. In two specimens that showed long segment atresia or total obliteration of the CBD (Figs. 5b, 6b) there was marked dilatation of the cystic duct. Specimens with multiple segments of atresia were often accompanied by large

gallbladders and occasionally, dilated cystic ducts. In contrast, one specimen at day 5 p.i. with only atresia at the distal end of the CBD had a small gallbladder (Fig. 1b). There was, however, no apparent association between the degree of extrahepatic biliary obliteration and age of the mice. The gallbladder and bile duct dilatation may represent an earlier phase of the disease or a genus-specific response to rotavirus infection.

In both the murine model and human BA, the disease is panbiliary, affecting both intrahepatic and extrahepatic biliary systems. Cystic dilatation of segments of the extrahepatic bile duct and the gallbladder is more prominent in the murine model; cystically dilated segments of the extrahepatic bile duct are seen infrequently in human BA [21, 22].

Conclusion

Although some differences exist between the rotavirus-infected Balb/c mouse liver model of BA and BA in humans, this murine model demonstrates the involvement of both intrahepatic and extrahepatic biliary systems, and is similar to the perinatal rather than the fetal form of human BA. The bile duct abnormalities seen in BA in the human are likely to be the end-result of heterogeneous etiologies [23] with perinatal viral infection being one of the triggers.

Acknowledgements The authors would like to thank Ms Caroline Ong and Ms Peizhen Hu for their help with tissue sectioning and staining.

References

1. Balistreri WF, Grand R, Hoofnagle JH (1996) Biliary atresia: current concepts and research directions. Summary of a symposium. Hepatology 23:1682–1692
2. Sokol RJ, Mack C, Narkewicz MR, Karrer FM (2003) Pathogenesis and outcome of biliary atresia. J Pediatr Gastroenterol Nutr 37:4–21
3. Riepenhoff-Talty M, Schaekel K, Clark HF, Mueller W, Uhnoo I, Rossi T, Fisher J, Ogra PL (1993) Group a rotaviruses produce extrahepatic biliary obstruction in orally inoculated newborn mice. Pediatr Res 33:394–399
4. Petersen C, Biermanns D, Kuske M, Schäkel K, Meyer-Junghänel, Mildenberger H (1997) New aspects in a murine model for extrahepatic biliary atresia. J Pediatr Surg 32:1190–1195
5. Petersen C, Grasshoff S, Luciano L (1998) Diverse morphology of biliary atresia in an animal model. J Hepatol 28:603–607
6. Vijayan V, Tan CEL (2000) Computer-generated three-dimensional morphology of the hepatic hilar bile ducts in biliary atresia. J Pediatr Surg 35:1230–1235
7. Nio M, Ohi R, Miyano T, Saeki M, Shiraki K, Tanaka K (2003) Five-and 10-year survival rates after surgery for biliary atresia: a report from the Japanese Biliary Atresia Registry. J Pediatr Surg 38:997–1000
8. Tsuchida Y, Kawarasaki H, Iwanka T, Uchida H, Nakanishi H, Uno K (1995) Antenatal diagnosis of biliary atresia (type 1 cyst) at 19 week's gestation: differential diagnosis and etiological implications. J Pediatr Surg 30:697–699
9. Hinds R, Davenport M, Mieli-Vergani G, Hadzic N (2004) Antenatal presentation of biliary atresia. J Pediatr 144:43–46
10. Desmet VJ (1992) Congenital diseases of intrahepatic bile ducts: variation on the theme "ductal plate malformation". Hepatology 16:1069–1083
11. Tan CEL, G Moscoso (1995) The developing human biliary system at the porta hepatis level between 11 and 25 weeks of gestation: a way to understanding biliary atresia—part two. Pathol Internat 44:600–610
12. Raweily EA, Gibson AAM, Burt AD (1990) Abnormalities of intrahepatic bile ducts in extrahepatic biliary atresia. Histopathology 17:521–527
13. Low Y, Vijayan V, Tan CEL (2001) The prognostic value of ductal plate malformation and other histologic parameters in biliary atresia: an immunohistochemical study. J Pediatr 139:320–322
14. Parashar K, Tarlow MJ, McCrae MA (1992) Experimental reovirus type 3-induced murine biliary tract disease. J Pediatr Surg 27:843–847
15. Ogawa T, Suruga K, Kojima Y, Kitahara T, Kuwabara N (1983) Experimental study of the pathogenesis of infantile obstructive cholangiopathy and its clinical evaluation. J Pediatr Surg 18:131–135
16. Czech-Schmidt G, Verhagen W, Szavay P, Leonhardt J, Petersen C (2001) Immunological gap in the infectious animal model for biliary atresia. J Surg Res 101:62–67
17. Azar G, Beneck D, Lane B, Markowitz J, Daum F, Kahn E (2002) Atypical morphologic presentation of biliary atresia and value of serial liver biopsies. J Pediatr Gastroenterol Nutr 34:212–215
18. Tan Kendrick AP, Phua KB, Ooi BC, Tan CEL (2003) Biliary atresia: making the diagnosis by the gallbladder ghost triad. Pediatr Radiol 33:311–315
19. Farrant P, Meire HB, Mieli-Vergani G (2000) Ultrasound features of the gall bladder in infants presenting with conjugated hyperbilirubinaemia. Br J Radiol 73:1154–1158
20. Park WH, Choi SO, Lee HJ (1999) The ultrasonographic 'triangular cord' coupled with gallbladder images in the diagnostic prediction of biliary atresia from infantile intrahepatic cholestasis. J Pediatr Surg 34:1706–1710
21. Lee HC, Yeung CY, Chang PY, Sheu JC, Wang NL (2000) Dilatation of the biliary tree in children: sonographic diagnosis and its clinical significance. J Ultrasound Med 19:177–182
22. Komuro H, Makino SI, Momoya T, Nishi A (2000) Biliary atresia with extrahepatic biliary cysts—cholangiographic patterns influencing the prognosis. J Pediatr Surg 35:1771–1774
23. Perlmutter DH, Shepherd RW (2002) Extrahepatic biliary atresia: a disease or phenotype? Hepatology 35:1297–1304